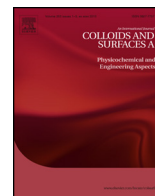




Contents lists available at ScienceDirect

# Colloids and Surfaces A: Physicochemical and Engineering Aspects

journal homepage: [www.elsevier.com/locate/colsurfa](http://www.elsevier.com/locate/colsurfa)

## Dielectric analysis of CMPS-supported ionic liquids (ILs) microspheres in model gasoline by means of dielectric relaxation spectroscopy



Mingjuan Han<sup>a</sup>, Mingyue Chen<sup>a</sup>, Hui Wan<sup>b</sup>, Xiaomeng Wang<sup>d</sup>, Jikui Wang<sup>a</sup>, Juan Wang<sup>c</sup>, Kongshuang Zhao<sup>c,\*</sup>, Guofeng Guan<sup>b,\*\*</sup>

<sup>a</sup> College of Sciences, Nanjing University of Technology, Nanjing, Jiangsu 210009, China

<sup>b</sup> College of Chemistry and Chemical Engineering, Nanjing University of Technology, Nanjing 210009, China

<sup>c</sup> College of Chemistry, Beijing Normal University, Beijing 100875, China

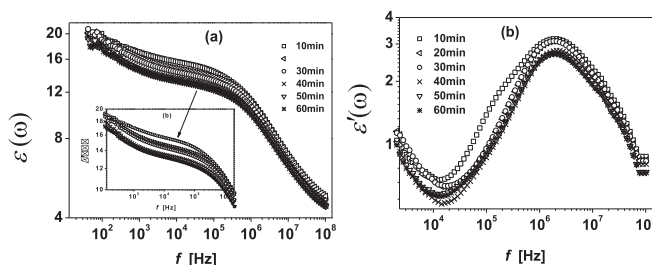
<sup>d</sup> The First Union Workshop of Sinopec Luoyang Company, China

### HIGHLIGHTS

- Real-time monitoring of dielectric measurements was performed by DRS.
- Dielectric parameters were obtained by fitting Cole–Cole equation to DRS data.
- Hanai method was employed to estimate the phase parameters.
- Dependences of the obtained parameters on the extractive time were investigated.
- Result of dielectric analysis was confirmed reasonable by interfacial electrokinetic model.

### GRAPHICAL ABSTRACT

Dependences of (a) permittivity  $\epsilon'(\omega)$  and (b) dielectric loss  $\epsilon''(\omega)$  spectra of suspension of CuCl/CMPS-Im(Cl) microspheres in model gasoline on extractive time.



### ARTICLE INFO

#### Article history:

Received 6 May 2013

Received in revised form 18 June 2013

Accepted 15 July 2013

Available online xxx

#### Keywords:

Dielectric relaxation spectroscopy (DRS)

Interfacial polarization

Real-time monitoring

Ionic liquids (ILs)

Thiophene

### ABSTRACT

Real-time monitoring of dielectric behaviors of CMPS-supported imidazolium ionic liquids (ILs) microspheres in model gasoline was performed by dielectric relaxation spectroscopy (DRS) from 40 Hz to 110 MHz. One dielectric relaxation in MHz frequency range is obviously observed for all systems and determined to be closely related to the interfacial polarization. The interfacial polarization is attributed from the different conductivities between dispersed microspheres and model gasoline since imidazolium-based ionic liquids have been immobilized on the surfaces of dispersed microspheres in the form of optimized spatial configurations. Meanwhile, dielectric parameters ( $\epsilon_1$ ,  $\kappa_1$ ,  $\epsilon_H$ ,  $\kappa_H$  and  $f_0$ ) for all the systems are obtained by fitting Cole–Cole equation to the dielectric data. From the dielectric parameters, Hanai equations are employed to calculate phase parameters ( $\phi$ ,  $\kappa_m$ ,  $\epsilon_p$  and  $\kappa_p$ ), which is used to characterize the electrical and structural properties of constituent phases of suspensions of conducting particles in non-conducting medium. The time-dependences of dielectric parameters and phase parameters are investigated in detail, and interfacial electrokinetic model for suspension of dense particles has been employed for interpreting these time-dependences. Here, we found that possible  $\pi$ -complexation bond and  $\pi$ - $\pi$  interaction between imidazole rings of ILs and thiophene are responsible for time-dependences of all parameters. Furthermore, the time-dependences of parameters indicate that the electron density (polarization strength) on surfaces of dispersed microspheres decreases with the increment of extraction time.

© 2013 Elsevier B.V. All rights reserved.

\* Corresponding author. Tel.: +86 010 58808283.

\*\* Corresponding author.

E-mail addresses: [zhaoks@bnu.edu.cn](mailto:zhaoks@bnu.edu.cn) (K. Zhao), [guangf@njut.edu.cn](mailto:guangf@njut.edu.cn) (G. Guan).

## 1. Introduction

Dielectric relaxation spectroscopy (DRS) is the most promising electrokinetic tool for colloidal suspensions because of its sensitivity to the interfacial charge distribution and its high sensitivity in the evaluation of electrical properties of interfaces [1,2]. Meanwhile, DRS is effective in situ and real-time investigation due to non-invasion and quick measurement [2]. It is well-known that colloidal suspensions are heterogeneous systems which exhibit different dielectric behaviors depending on the frequency of the applied field [3,4]. Microwave dielectric measurements (over the frequency range of  $10^5$ – $10^{10}$  Hz) have been used to estimate the dynamics of bound water molecules and counterions in many types of polymers, biopolymers and inorganic colloids [5–7]. Dielectric measurement in the radio frequency interval (over the frequency range of  $10^{-4}$ – $10^8$  Hz) is often employed to investigate the information of interfaces, meanwhile, theories on the dielectric properties of colloidal suspensions are commonly ascribed to the most typical relaxation mechanisms, such as the Maxwell–Wagner–O’Konski (MWO) polarization relaxation [8–10] (typically at MHz) and counterion polarization relaxation [11–13] (typically at kHz). Accordingly, these theories are applied to predict the appearance of phenomena of polarization, conduction and charge diffusion, interfacial configuration, and so on [14–16]. Analytical theories on the dielectric properties of colloidal suspensions require ideal systems with homogeneous distribution of dispersed particles since dielectric measurements inform about a collective response of the system. Over the past three decades, the heterogeneous systems, such as colloidal particles [17–19], microemulsions [20], vesicles [21] and biological cell dispersions [22], have been studied. Especially, particles in conducting medium, where charged particles were dispersed in aqueous solution, have been widely studied experimentally [23–26], theoretically [27–30] and numerically [31,32] by dielectric relaxation method. However, until recently, there is little information on the dielectric properties of suspensions of conducting particles in non-conducting medium although researchers have reported dielectric properties of water-in-oil (micro)emulsions containing oil, water and surfactants by means of DRS [16]. Then, an ideal and well-constructed system of conducting particles in non-conducting medium is so attractive to us.

It is well-known that effort to make existing separation methods more efficient and eco-friendly may get a boost from a relatively new class of solvents known as ionic liquids (ILs). Supporting ILs moieties on  $\text{SiO}_2$ , PS and resins [33–38] is a method to overcome the difficult procedures for product purification and regeneration of ILs in separation process, together with the high cost and loss of ILs in their industrial application. We have devoted to improve new adsorbed materials for the desulfurization performances of CMPS-supported imidazole-based ILs microspheres in 2012 [39]. Understanding the characteristics of the solid–liquid interface [40] may lead to suitable designs for adsorbed materials. Accordingly, an understanding of an ideal system (CMPS supported-ILs microspheres) of adsorbed materials, such as thermal conductivity, dielectric property, and complex dynamics between supported-ILs and thiophene, is necessary.

Therefore, as an extension of the previous work carried out by our group, real-time monitoring of dielectric properties of CMPS-supported imidazole-based ILs in model gasoline has been carried out in the frequency range from 40 Hz to 110 MHz. The relaxation mechanism was discussed in terms of interfacial polarization theory. Furthermore, dielectric parameters were obtained by fitting experimental data with Cole–Cole equation to gain an opportunity to briefly elucidate the differences or similarities of suspensions between conducting particles in non-conducting medium and non-conducting particles in conducting medium.

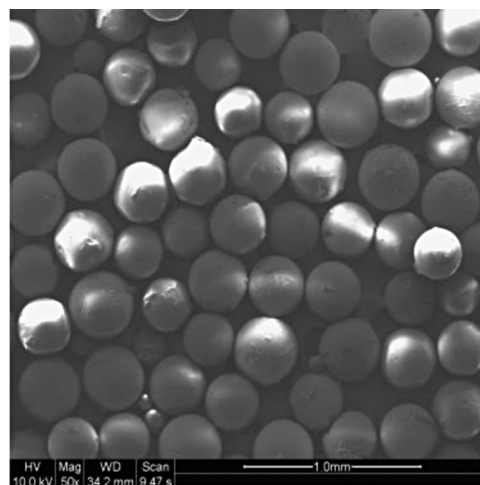


Fig. 1. SEM image of chloromethylated polystyrene (CMPS) microspheres.

Meanwhile, phase parameters characterizing the electric and structural properties of the constituent phases (CMPS-supported ILs and model gasoline medium) were calculated using Hanai equation. Companion with interfacial electrokinetic model for densely packed sediments, more discussion has been placed on the extractive time-dependence of phase parameters of CMPS-supported imidazole-based ILs to elucidate the electrokinetic characteristic of suspension of conducting particles in non-conducting medium.

## 2. Materials and methods

### 2.1. Materials

The particles in model gasoline are spherical chloromethylated polystyrene (CMPS), CMPS-Im(Cl) (immobilizing of N-methylimidazole onto CMPS), and a series of CMPS-supported metal chlorides ILs ( $\text{CuCl}$ ,  $\text{FeCl}_3$  and  $\text{ZnCl}_2$ /CMPS-Im(Cl)) (immobilizing of metal chlorides on the CMPSIm(Cl)). The SEM image of CMPS microspheres shown in Fig. 1 is extracted from our previous work [39], and it shows that the radii of particles are in the range of 250–300  $\mu\text{m}$ . Before dielectric measurements, the particles are purified by using the high-velocity centrifugal machine and washed with methanol and ethanol for 6 times, separately, and then they are dried in a vacuum oven at 50 °C for 24 h. It should be noted that the excessive metal chlorides adsorbed on the microspheres physically are easily removed by washing with methanol and ethanol since metal chlorides have high solubility in them.

### 2.2. Preparation of model gasoline

Model gasoline was composed of thiophene and n-octane. 0.6342 g thiophene was accurately weighed and added into 250 mL volumetric flask, then n-octane was added into the above volumetric flask until the volume was determined at 250 mL. The concentration of thiophene (sulfur content) was 1381 ppm (ppm was mass fraction) in model gasoline.

### 2.3. Dielectric measurement

Dielectric measurements were carried out in frequency range from 40 Hz to 110 MHz on an HP 4294A with Precision Impedance Analyzer (Agilent Technologies), which is tested and calibrated in accordance with the procedure recommended by the manufacturer. The amplitude of the applied alternating current (AC) field was 500 mV, and the measurement of temperature was  $30 \pm 1$  °C.

The dielectric measurement cell with concentric cylindrical platinum electrodes was employed, which has been described in previous works [41,42]. The solution volume used in the experiment was 2 mL in order to submerge the electrodes. All the experimental data were subjected to certain corrections for errors arising from stray capacitance ( $C_r$ ) and cell constant ( $C_l$ ) [43], which were determined by using several standard liquids, such as pure water, methanol, ethanol and acetone, respectively. The residual inductance  $Lr$  due to the cell assembly and the terminal leads will make errors, so  $Lr$  of the dielectric cell was determined by use of standard KCl solutions with different concentrations. Then, the permittivity and conductivity were calculated from the corrected capacitance and conductance based on the Eqs. (1)–(4).

$$C_s = \frac{C_x(1 + \omega^2 LrC_x) + LrG_x^2}{(1 + \omega^2 LrC_x)^2 + (\omega LrG_x)^2} - Cr \quad (1)$$

$$G_s = \frac{G_x}{(1 + \omega^2 LrC_x)^2 + (\omega LrG_x)^2} \quad (2)$$

$$\varepsilon = \frac{C_s - Cr}{C_l} \quad (3)$$

$$\kappa = \frac{G_s \varepsilon_0}{C_l} \quad (4)$$

where  $C_x$ ,  $G_x$ ,  $C_s$  and  $G_s$  are the measured and corrected capacitance/conductance, respectively,  $\omega (= 2\pi f)$  is the angular frequency,  $Cr$  is the stray capacitance,  $C_l$  is the cell constant, and  $Lr$  is the stray inductance,  $\varepsilon_0$  is the permittivity of vacuum equal to  $8.8541 \times 10^{-12} \text{ F m}^{-1}$ ,  $\varepsilon$  and  $\kappa$  are the permittivity and conductivity, respectively.

#### 2.4. Determination of dielectric parameters

The dielectric relaxation parameters were obtained by fitting the following equation including one ( $i=1$ ) or two ( $i=1,2$ ) Cole–Cole's terms [44] to experimental dielectric spectra:

$$\varepsilon^* = \varepsilon' - j\varepsilon'' = \varepsilon_h + \sum_i \frac{\Delta\varepsilon_i}{1 + (j\omega\tau_i)^{\beta_i}} \quad (5)$$

where  $\varepsilon'' = (\kappa - \kappa_l)/\omega\varepsilon_0$ ,  $\kappa_l$  is the low-frequency limit of conductivity,  $\varepsilon_h$  is the high-frequency limit of relative permittivity,  $\Delta\varepsilon$  is the relaxation intensity,  $\tau (= 1/(2\pi f_0))$ ,  $f_0$  is the characteristic relaxation frequency) is the characteristic relaxation time, and  $\beta$  is the Cole–Cole parameter ( $0 < \beta \leq 1$ ).  $\omega (= 2\pi f)$  is the angular frequency. In this work, the particles are conductive and thus there is a considerable electrode polarization (EP) effect [16] due to the accumulation of spatial charge at the electrode–gasoline interface. Then, the electrode polarization term is added to Eq. (5) as

$$\varepsilon^* = \varepsilon' - j\varepsilon'' = \varepsilon_h + \sum_i \frac{\Delta\varepsilon_i}{1 + (j\omega\tau_i)^{\beta_i}} + A\omega^{-m} \quad (6)$$

where  $A$  and  $m$  in the electrode polarization term are adjustable parameters.

Meanwhile, the logarithmic derivative (LD) method is used to optimize the fitting, which showed an excellent representation of the true imaginary part of the permittivity,  $\varepsilon''(\omega)$ , and turned out to be very effective in resolving overlapped relaxations [45,46], namely,

$$\varepsilon''_{LD}(\omega) = -\frac{\pi}{2} \frac{\partial \varepsilon''}{\partial \ln \omega} \approx \varepsilon''_{rel}(\omega) \quad (7)$$

where  $\varepsilon''_{LD}$  and  $\varepsilon''_{rel}$  denote the derivative dielectric loss of real permittivity  $\varepsilon'(\omega)$  and the dielectric loss deduced from dc conductivity, respectively.

According to LD method, one dielectric relaxation in this work dominates in all investigated systems. Then, dielectric parameters, listed in Tables 1 and 2, are obtained by fitting Eq. (6) to the experimental data.  $\kappa_l$  is determined by using equation  $\kappa = \omega\varepsilon_0\varepsilon'' + \kappa_l$  [47] to fit the experimental data of conductivity according to dielectric parameters (i.e.  $\varepsilon_l$ ,  $\varepsilon_h$ ,  $\beta$ ,  $f_0$ ) obtained by curve-fitting of real part of Eq. (6) to the experimental data. Then,  $\kappa_h$  are calculated by using the equation [48]

$$\kappa_h = ((\varepsilon_l - \varepsilon_h) \times 2 \times \pi \times f_0 \times \varepsilon_0) + \kappa_l \quad (8)$$

the calculated values of  $\kappa_h$  in Eq. (8) well agree with that estimated by fitting the experimental data of conductivity with the equation  $\kappa = \omega\varepsilon_0\varepsilon'' + \kappa_l$  [47].

#### 2.5. Determination of phase parameters

For densely packed sediments of particles-in-oil, where conductive spherical particles with the radii of 250–300  $\mu\text{m}$  are dispersed in model gasoline, we may assume that the conductivity of model gasoline is much lower than that of conductive particles. Here we will introduce Hanai equation [49] for concentrated system into our dielectric analysis, this equation was an extension of Wagner's equation [9] to high volume fractions along the Bruggeman's effective medium approach [50],

$$\frac{\varepsilon^* - \varepsilon_p^*}{\varepsilon_m^* - \varepsilon_p^*} \left( \frac{\varepsilon_m^*}{\varepsilon^*} \right)^{1/3} = 1 - \phi \quad (9)$$

where  $\varepsilon_p^* (\varepsilon_p^* = \varepsilon_p - j\kappa_p/\omega\varepsilon_0)$  and  $\varepsilon_m^* (\varepsilon_m^* = \varepsilon_m - j\kappa_m/\omega\varepsilon_0)$  are the complex relative permittivities of particles and medium, respectively, and  $\phi$  is the volume fraction. Since we can assume  $\kappa_p \geq \kappa_m$  for spherical conductive particles in model gasoline, phase parameters ( $\phi$ ,  $\varepsilon_p$ ,  $\kappa_p$  and  $\kappa_m$ ) [41,49] are approximately determined by the dielectric relaxation parameters ( $\varepsilon_l$ ,  $\varepsilon_h$ ,  $\kappa_l$  and  $\kappa_h$ ) on the basis of the M–W relaxation (this relaxation is of interest here), as shown in Eqs. (10)–(13).

$$\phi = 1 - \left( \frac{\varepsilon_m}{\varepsilon_l} \right)^{1/3} \quad (10)$$

$$\varepsilon_p = \varepsilon_m + \frac{\varepsilon_h - \varepsilon_m}{1 - (\varepsilon_h/\varepsilon_l)^{1/3}} \quad (11)$$

$$\kappa_p = \kappa_h + \frac{3 - (2 + \varepsilon_m/\varepsilon_h)(\varepsilon_h/\varepsilon_l)^{1/3}}{3[1 - (\varepsilon_h/\varepsilon_l)^{1/3}]^2} \quad (12)$$

$$\kappa_m = \kappa_l(1 - \phi)^3 \quad (13)$$

Using these equations, we can determine the volume fraction  $\phi$  of the conductive particles, the conductivity  $\kappa_m$  of the model gasoline, and the relative permittivity  $\varepsilon_p$  and conductivity  $\kappa_p$  of the conductive particles from the dielectric relaxation parameters if the relative permittivity  $\varepsilon_m$  of the model gasoline was given.

### 3. Results and discussion

#### 3.1. Dependences of dielectric behaviors on drying time

Because ILs are organic salts with melting points around or below ambient temperature, they can easily adsorb water molecule from the atmosphere due to their polarities. In order to eliminate the influence of adsorbed water on the dielectric behavior, the drying time-dependences of dielectric behaviors of all CMPS-supported metal chlorides ILs microspheres are investigated. The result shows that the influence can be eliminated completely when the samples are dried at 45 °C for corresponding hours. Fig. 2

**Table 1**

Dielectric parameters of suspensions of CMPS-supported metal chlorides ILS microspheres dispersed in model gasoline. Notes:  $\Delta\varepsilon$  and  $f_0$  are the permittivity increments and the characteristic relaxation time, defined as  $\Delta\varepsilon = \varepsilon_h - \varepsilon_l$  and  $f_0 = 1/(2\pi\tau_0)$ , respectively.  $A$  and  $m$  are adjustable parameters.

Samples	Dielectric parameters						
	$\varepsilon_l$	$\varepsilon_h$	$\Delta\varepsilon$	$\beta$	$f_0$	$A$	$m$
CMPS	–	–	–	–	–	–	–
CMPS-Im(Cl)	10.10	1.90	8.20	0.71	2,891,523	66	0.53
CuCl/CMPS-Im(Cl)	15.90	4.10	11.80	0.58	1,867,822	90	0.48
ZnCl <sub>2</sub> /CMPS-Im(Cl)	8.25	3.10	5.15	0.40	64,519	590	0.58
FeCl <sub>3</sub> /CMPS-Im(Cl)	3.90	3.10	0.80	0.70	241,519	66	0.53

**Table 2**

Dielectric parameters of suspension of CuCl/CMPS-Im(Cl) microspheres dispersed in model gasoline during the extractive time from 10 min to 60 min. Notes:  $\Delta\varepsilon$  and  $\tau_0$  are the permittivity increment and the characteristic relaxation time, defined as  $\Delta\varepsilon = \varepsilon_h - \varepsilon_l$  and  $\tau_0 = 1/(2\pi f_0)$ , respectively.

Extractive time (min)	Dielectric parameters						
	$\varepsilon_l$	$\varepsilon_h$	$\Delta\varepsilon$	$\beta$	$\kappa_l$ ( $\mu\text{S/m}$ )	$f_0$ (Hz)	$\tau_0$ (s)
10	15.90	4.10	11.80	0.58	0.35	1,867,822	$8.5252 \times 10^{-8}$
20	15.10	4.00	11.10	0.57	0.41	1,965,665	$8.1009 \times 10^{-8}$
30	14.45	3.75	10.70	0.56	0.42	2,099,703	$7.5837 \times 10^{-8}$
40	14.00	3.70	10.30	0.55	0.44	2,158,001	$7.3788 \times 10^{-8}$
50	13.50	3.60	9.90	0.54	0.46	2,247,887	$7.0838 \times 10^{-8}$
60	13.50	3.60	9.90	0.54	0.46	2,247,887	$7.0838 \times 10^{-8}$

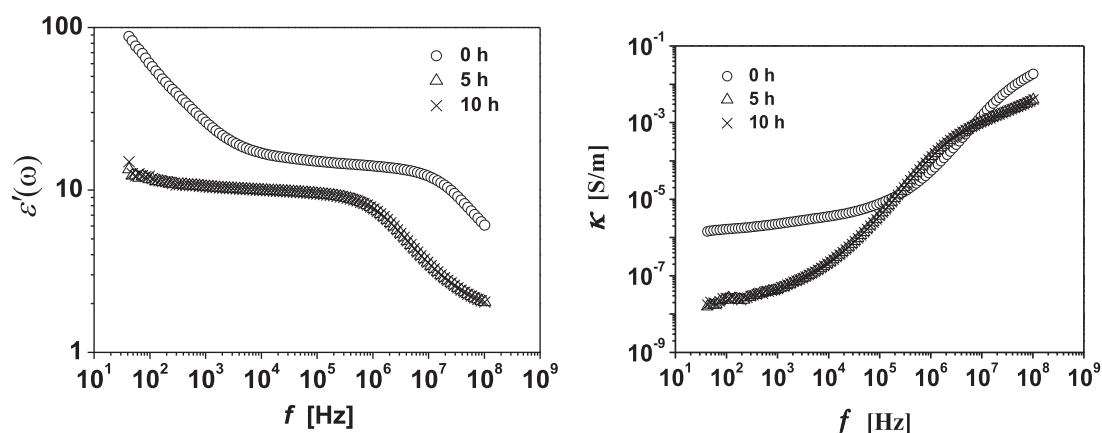


Fig. 2. The recorded DRS of suspensions of dried CMPS-Im(Cl) microspheres in a vacuum oven at 45 °C for 0 h, 5 h, 10 h, separately.

gives an example of the recorded spectra of suspensions of CMPS-Im(Cl) microspheres in model gasoline, and it should be noted that CMPS-Im(Cl) microspheres under investigation were dried in a vacuum oven at 45 °C for 0 h, 5 h, 10 h, separately. As shown in Fig. 2, it can be seen that, when the samples are dried from 0 h to 5 h, both permittivity  $\varepsilon'$  and conductivity  $\kappa$  spectra of suspensions of the sample in model gasoline are much less than those of the sample without drying, and then the spectra are kept constant when the drying time varies from 5 h to 10 h. This change of dielectric behavior denotes that the accuracy and reproducibility of investigated DRS for this sample can be realized when the sample is dried at 45 °C in a vacuum oven for more than 5 h. Therefore, all samples for dielectric measurement are dried at 45 °C in a vacuum oven for corresponding hours determined by DRS.

### 3.2. Comparison of dielectric behaviors of colloidal suspensions

Fig. 3 shows the frequency dependence of permittivity  $\varepsilon'$  and dielectric loss  $\varepsilon''$  from 40 Hz to 110 MHz for CMPS, CMPS-Im(Cl) and M/CMPS-Im(Cl) (M = CuCl, ZnCl<sub>2</sub> and FeCl<sub>3</sub>) ILS microspheres in model gasoline. It is well-known that suspensions in electrolyte solutions are characterized by two typical relaxation mechanisms, low-frequency (LF) relaxation and Maxwell–Wagner (M–W) relaxation, both of the two mechanisms are closely related to the

polarization of electrical double electric layer of dispersed particles. The low-frequency relaxation (typically at kHz) was first given a theoretical explanation (surface diffusion mechanism, SDM) by Schwarz [11] by assuming counterions move only along the particle surface without exchanging with the bulk electrolyte ions. Then, Dukhin and Shilov [12,13] proposed that LF relaxation was associated with the buildup of ionic concentration gradient around particles (volume diffusion mechanism, VDM). Since colloidal suspensions possessed interfaces with different electrical properties, namely  $\kappa_p/\varepsilon_p \neq \kappa_m/\varepsilon_m$  (subscripts  $p$  and  $m$  denote particle and medium, respectively), then the buildup of charges on the interfaces led to M–W relaxation [8,9]. Subsequently, this relaxation was extended by O’Konski [10] by taking into account the surface conductivity without any specification of its physical nature.

Based on the above introduction, we concluded that no so-called LF relaxation was observed over the low frequency range of 40 Hz–10<sup>5</sup> Hz. This is because imidazolium (Im) ILS and its counterions on the surfaces of dispersed particles cannot freely dissociate into the inside of model gasoline, meanwhile, they can only stand at the interfaces in the form of different optimized spatial structures of counterion-CMPS-Im(Cl) complexes by covalent bond [39]. Meanwhile, we can attribute the relaxations in this work to the M–W polarization relaxations because of the different electrical properties between dispersed particles and model gasoline. As for

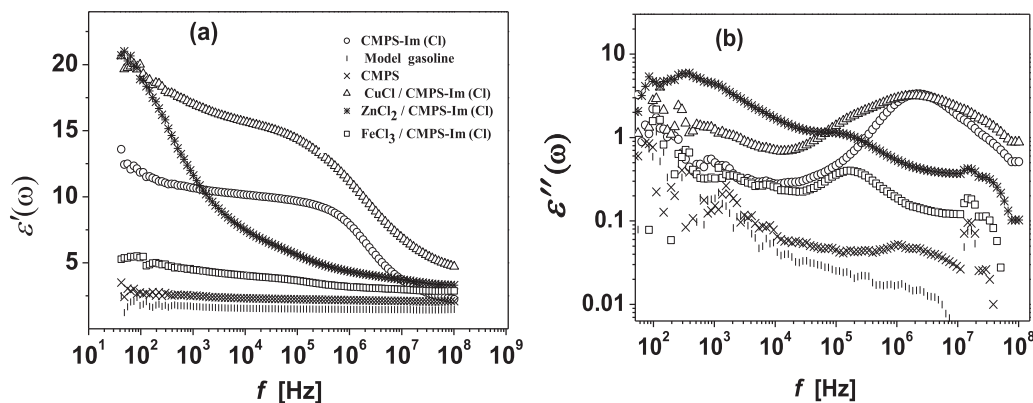


**Fig. 3.** Frequency dependences of (a) permittivity  $\varepsilon'(\omega)$  and (b) dielectric loss  $\varepsilon''(\omega)$  spectra of model gasoline and suspensions of CMPS, CMPS-Im(Cl), CuCl/CMPS-Im(Cl), ZnCl<sub>2</sub>/CMPS-Im(Cl) and FeCl<sub>3</sub>/CMPS-Im(Cl) microspheres dispersed in model gasoline.

the systems in this work, the reason for the M–W polarization relaxation is the buildup of charges on the interfaces are caused by the different optimized spatial structures of CuCl<sub>2</sub><sup>-</sup>, ZnCl<sub>3</sub><sup>-</sup> and FeCl<sub>4</sub><sup>-</sup>-CMPS-Im(Cl) complexes at the interfaces [51,52]. This phenomenon for the systems in model gasoline is much different from the traditional electrical double layer of aqueous solution that always investigated [17–32].

According to the determination of dielectric parameters described in the dielectric spectra of Section 2.4, the Cole–Cole formula with one-dispersion term and the contribution of electrode polarization ( $A\omega^{-m}$ ) is used to fit the dielectric experimental data one by one. Then, dielectric parameters are obtained, and the best-fitting results are listed in Table 1. Table 1 shows relaxation parameters for the systems composed of CMPS-Im(Cl), CuCl/CMPS-Im(Cl), ZnCl<sub>2</sub>/CMPS-Im(Cl) and FeCl<sub>3</sub>/CMPS-Im(Cl) microspheres dispersed in gasoline.

First of all, as shown in Table 1, it should be pointed out that the values of Cole–Cole parameter  $\beta$  for all samples are much smaller than 1, which is not welcome in the aqueous colloidal suspensions since the relaxation cannot be considered as Debye type of relaxation (which is called as single relaxation mechanism). Here, we think the  $\beta$  values are reasonable, the detailed explanation is as follows: the surface of CMPS-Im(Cl) microspheres in model gasoline are possessed by imidazolium (Im) group and its counterions (CuCl<sub>2</sub><sup>-</sup>, ZnCl<sub>3</sub><sup>-</sup> and FeCl<sub>4</sub><sup>-</sup>) by mean of covalent bond [39]. Thus, the interfacial electric properties are obviously affected by optimized spatial configurations of both imidazolium (Im) group and its counterions. Accordingly, when the AC field is applied, imidazolium (Im) group and its corresponding counterions require different time to restore the equilibrium charge distribution of surface of dispersed particles, and the required time is called the characteristic relaxation time  $\tau_0$  in dielectric analysis. Therefore, the values of  $\beta$  for each sample are much smaller than 1 due to the broader distribution of relaxation time. Here, in aqueous colloidal suspensions, when the values of  $\beta$  for all samples are much smaller than 1, and we think it is multi-relaxation mechanisms since only anions and cations freely move with the AC field, and the time for them to restore the equilibrium charge distribution of surface of dispersed particles is not much different. As for the above phenomenon, it indicates that the distribution of  $\tau_0$  obtained from suspensions of conducting particles in non-conducting medium is much different from the aqueous solution that always investigated [17–32].

Second, the relaxation frequency is 2,891,523 Hz for CMPS-Im(Cl) microspheres in model gasoline, after further immobilizing CuCl, ZnCl<sub>2</sub> and FeCl<sub>3</sub> metal chlorides onto the surface of CMPS-Im(Cl), then the characteristic relaxation frequencies  $f_0$  of these systems are shifted to 1,867,822 Hz, 64,519 Hz and 241,519 Hz, respectively, namely shifted to the lower relaxation frequencies.

$f_0 (= 1/(2\pi\tau_0))$  is related to the required time for restoring the equilibrium charge distribution of surfaces of dispersed particles along with the applied field. Therefore, as for the samples of CMPS-Im(Cl) and M/CMPS-Im(Cl) (M = CuCl, ZnCl<sub>2</sub> and FeCl<sub>3</sub>), the different spatial structures of CuCl<sub>2</sub><sup>-</sup>, ZnCl<sub>3</sub><sup>-</sup> and FeCl<sub>4</sub><sup>-</sup>-CMPS-Im(Cl) complexes [51,52] on the surface of particles are responsible for the shift of characteristic relaxation frequency  $f_0$ . Meanwhile, different dielectric increments  $\Delta\varepsilon$  can be observed for the systems in Table 1, which is also due to the different optimized spatial structures of dispersed particles in model gasoline.

### 3.3. Dependences of dielectric behaviors of CMPS-supported ILs in model gasoline on extraction time

#### 3.3.1. Dependences of dielectric behaviors of CuCl/CMPS-Im(Cl) ILs in model gasoline on extraction time

Fig. 4 shows dependences of permittivity  $\varepsilon'(\omega)$ , dielectric loss  $\varepsilon''(\omega)$  and conductivity  $\kappa(\omega)$  spectra of CuCl/CMPS-Im(Cl) microspheres on the extraction time (from 10 min to 60 min). Only the recorded spectra from 10 min to 6 h are extracted from all displayed spectra and displayed in Fig. 4 because the spectra do not vary when the extraction time is longer than 50 min. One dielectric relaxation has been confirmed by dielectric analysis described in Section 3.2. Accordingly, as described in Section 2.4, the Cole–Cole formula including one Cole–Cole's term and electrode polarization term ( $A\omega^{-m}$ ) is used to fit the experimental data and the best-fitting results are listed in Table 2.

As for dependences of dielectric parameters  $\Delta\varepsilon$  and  $\tau_0$  on extraction time, it can be obviously seen from Fig. 5 and Table 2 that  $\Delta\varepsilon$  and  $\tau_0$  sharply decrease within 50 min, then both of them are kept invariant with the increment of extraction time. First, the reason for such phenomenon, dielectric increment  $\Delta\varepsilon$  sharply decreases with the increment of extraction time within 50 min, may be explained as: a possible  $\pi$ – $\pi$  interaction (between thiophene and imidazole rings of ILs bonded on the surfaces of CMPS microspheres) is performed [53,54], and the possible  $\pi$ –complexation bond between CuCl/CMPS-Im(Cl) microspheres and thiophene is formed by means of d– $\pi^*$  back-donation of electrons from 3d orbitals of copper(I) to  $\pi^*$  orbitals of thiophene [51,52,55]. Both of  $\pi$ – $\pi$  interaction and  $\pi$ –complexation bond will weaken the electron density of surface of CuCl/CMPS-Im(Cl) microspheres in model gasoline. Therefore, the induced dipole moment as a result of the asymmetric distribution of charges around CuCl/CMPS-Im(Cl) microspheres decreases with the extraction time, namely, the polarization strength at the interface between CuCl/CMPS-Im(Cl) microspheres and model gasoline decreases. Accordingly, this result manifested by dielectric increment is:  $\Delta\varepsilon$  decreases with the increment of extraction time. Second, the characteristic relaxation

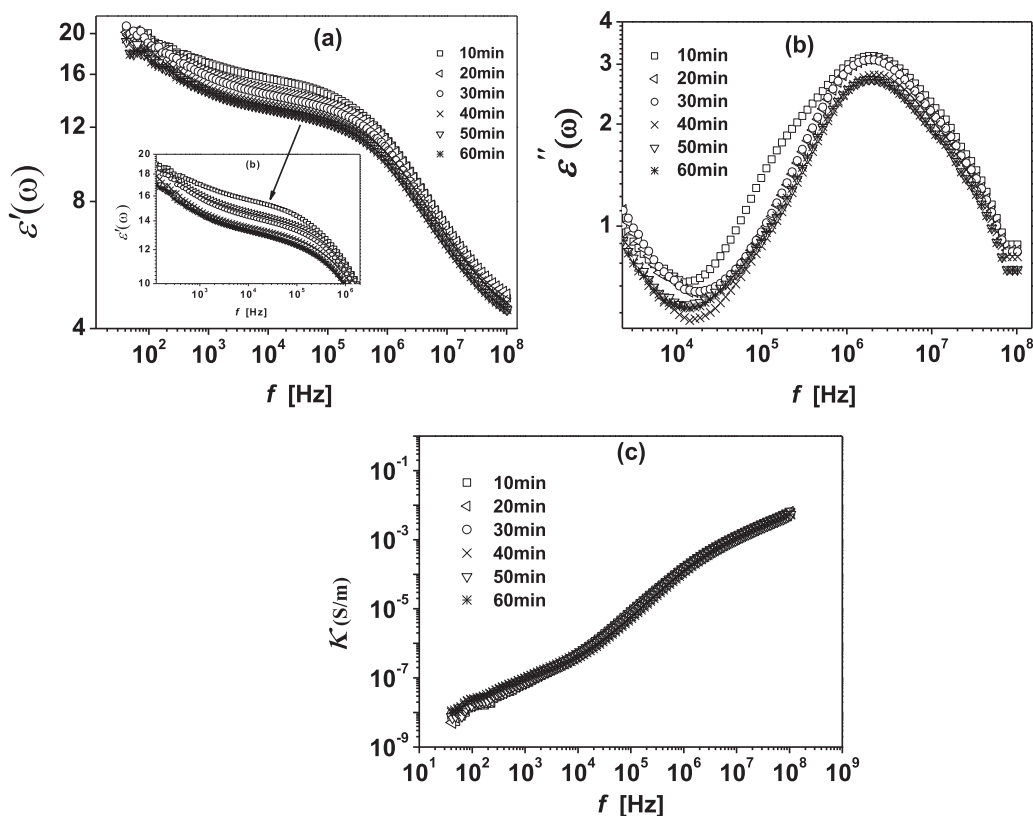


Fig. 4. Dependences of (a) permittivity  $\varepsilon'(\omega)$ , (b) dielectric loss  $\varepsilon''(\omega)$  and (c) conductivity  $\kappa(\omega)$  spectra of suspension of CuCl/CMPS-Im(Cl) microspheres in model gasoline on extractive time.

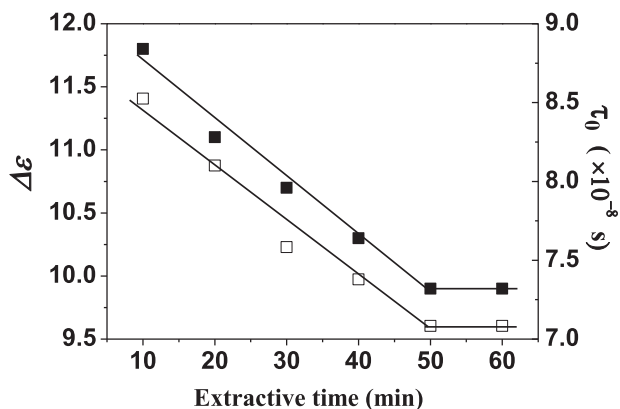


Fig. 5. Dielectric increment  $\Delta\varepsilon$  ■ and relaxation time  $\tau_0$  □ plotted as a function of extractive time using CuCl/CMPS-Im(Cl) ILS to extract thiophene from model gasoline. The solid line is only to guide the eyes.

time  $\tau_0$  decreases with increasing extraction time within 50 min, obviously. It is well-known that  $\tau_0$  is the time required for restoring the equilibrium charge distribution around the CuCl/CMPS-Im(Cl) microspheres when the AC field is applied. Therefore, dependence of relaxation time  $\tau_0$  on extraction time within 50 min indicates that the required time to restore the equilibrium charge distribution decreases. The reason for this is: the charges density on the surface of the CuCl/CMPS-Im(Cl) microspheres is distributed better and better when more and more thiophene is extracted from model gasoline onto the interfaces. Third,  $\Delta\varepsilon$  and  $\tau_0$  are kept invariant when the extraction time is longer than 50 min. It means that dielectric property of the system does not vary with the increment of extraction time because the charges density on the surface of

CuCl/CMPS-Im(Cl) microspheres is distributed to the limit state when the extraction time is longer than 50 min.

Phase parameters calculated by Hanai method has been used as a rough estimate to predict the electrical properties of colloidal suspensions. Table 3 displays the electrical phase parameters ( $\phi$ ,  $\kappa_m$ ,  $\varepsilon_p$  and  $\kappa_p$ ) of suspension of CuCl/CMPS-Im(Cl) microspheres in model gasoline.  $\varepsilon_m$  is 1.4 (measured value) obtained from model gasoline. First, it can be seen from Table 3 that  $\varepsilon_p$  decreases, however,  $\kappa_p$  and  $\kappa_m$  increase with the increment of extraction time. This can be interpreted as follows: the possibility for extracting thiophene from model gasoline to interfaces is due to the two performances of  $\pi$ - $\pi$  interaction [53,54] and  $\pi$ -complexation bond [51,52,55] between dispersed microspheres and model gasoline. When more and more thiophene is extracted to the interfaces, these two performances will result in the decrement of electron density on surface of CuCl/CMPS-Im(Cl) microspheres in model gasoline, namely, the decrement of dipole moment (i.e. polarization strength). When the change of polarization strength is magnified by phase parameters, it is  $\varepsilon_p$  decreases, however,  $\kappa_p$  and  $\kappa_m$  increase with the increment of extraction time. Second, volume fraction  $\phi$  of CuCl/CMPS-Im(Cl) microspheres in model gasoline of per unit volume decreases with the increment of extraction time. The reason for this phenomenon is as follows: CuCl/CMPS-Im(Cl) microspheres in model gasoline possess the “hairy” surface imagined in Fig. 6 when CuCl/CMPS-Im(Cl) microspheres were dispersed in model gasoline, which is due to the immobilization of N-methylimidazole group and CuCl group onto the surface of CMPS [39]. As for densely packed sediment, these surface hairs (the “packed hairy” state) are kept close to the surface of CuCl/CMPS-Im(Cl) microspheres since they cannot well form similar dominant intermolecular attraction with model gasoline. According to DLVO theory [56], the suspension of densely packed sediments is much different from the dilute suspension. As for suspensions of dense particles in aqueous

**Table 3**  
Electrical phase parameters ( $P$ ,  $\kappa_m$ ,  $\varepsilon_p$  and  $\kappa_p$ ) of suspension of CuCl/CMPS-Im(Cl) microspheres in model gasoline determined from dielectric relaxation parameters ( $\kappa_l$ ,  $\varepsilon_l$ ,  $\varepsilon_h$  and  $\kappa_h$ ) measured at  $30 \pm 1$  °C. Notes: The value of  $\varepsilon_m$  is assumed to be 1.4 at  $30 \pm 1$  °C.

Extractive time (min)	Dielectric parameters				Phase parameters			
	$\varepsilon_l$	$\varepsilon_h$	$\kappa_l$ ( $\mu\text{S/m}$ )	$\kappa_h$ (S/m)	$\phi$	$\varepsilon_p$	$\kappa_p$ (S/m)	$\kappa_m$ ( $\mu\text{S/m}$ )
10	15.90	4.10	0.35	0.00123	0.5551	8.83	0.00467	0.0308
20	15.10	4.00	0.41	0.00121	0.5474	8.67	0.00471	0.0371
30	14.45	3.75	0.42	0.00125	0.5407	7.88	0.00472	0.0407
40	14.00	3.70	0.44	0.00124	0.5358	7.81	0.00473	0.0430
50	13.50	3.60	0.46	0.00124	0.5302	7.57	0.00475	0.0467
60	13.50	3.60	0.46	0.00124	0.5302	7.57	0.00475	0.0467

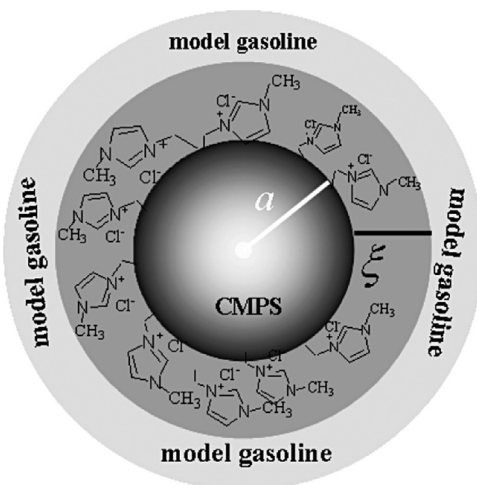


**Fig. 6.** Schematic illustration of interfacial structure of CMPS-Im(Cl) microspheres dispersed in model gasoline. Notes: CMPS is represented by the sphere with radius  $a$ , the dark shadow outside the sphere denotes the space where the optimized space structure of bounded imidazolium and its counterions on the boundary surfaces of CMPS particles. It should be noted that the dark shadow outside the CMPS sphere is a magnified picture, in fact it is a thin electrical layer outside the CMPS sphere.

solution, the electrochemical interaction between dispersed particles effectively appears when their separation is of the order of  $\lambda_D$  (Debye length, the effective thickness of electric double layer), approximately. Fig. 7(a) and (b) display the sketches for elucidating the interfacial interaction of two smooth particles (a) and rough particles (b) in aqueous solution, respectively. For two particles

with radius  $\alpha$  in aqueous solution, as shown in aqueous solution Fig. 7(a) and (b), the characteristic interaction region between them is a sphere with a radius  $(\alpha\lambda_D)^{1/2}$ , and a shadow is the interaction region of electric double layer, the characteristic dimension  $2\lambda_D$ . Although the system under our investigation, suspension of CuCl/CMPS-Im(Cl) microspheres about 250–300  $\mu\text{m}$  radii in model gasoline, is not aqueous solution, it belongs to the densely packed sediment. So, the interaction region between two particles is objectively existed just like the suspensions of dense particles in aqueous solution. Accordingly, when thiophene is gradually extracted from model gasoline to the surface of CuCl/CMPS-Im(Cl) microspheres to form complexes, the “packed hairy” state, as shown in Fig. 7(a) and (b) (where  $\overline{AB}$  represents the distance between two particles), is changed to the “expanded hairy” state (as shown in Fig. 7(c)) due to the intrusion of thiophene from the model gasoline to the interfaces. This behavior leads to the larger distance (shown by  $\overline{AB}$  in Fig. 7(c)) than the one (shown by  $\overline{AB}$  in Fig. 7(b)) between two particles, meanwhile, it also leads to the smaller interaction region of EDL (shown by the gray shadow in Fig. 7(c)). Correspondingly, the larger distance between two particles results in the fact: volume fraction  $f_0$  of CuCl/CMPS-Im(Cl) microspheres in model gasoline of per unit volume decreases with the increment of extraction time, shown in Table 3. Third, we pay more attention to the accuracy of Hanai method to predict phase parameters. It is well-known that water-in-oil emulsions have been extensively studied by dielectric spectroscopy and provided good test systems to examine the validity of Hanai equations [41,48,50]. The system under our investigation, the system of CuCl/CMPS-Im(Cl) microspheres dispersed in model gasoline, satisfies the situation of  $\kappa_p \geq \kappa_m$  since the surfaces of dispersed microspheres

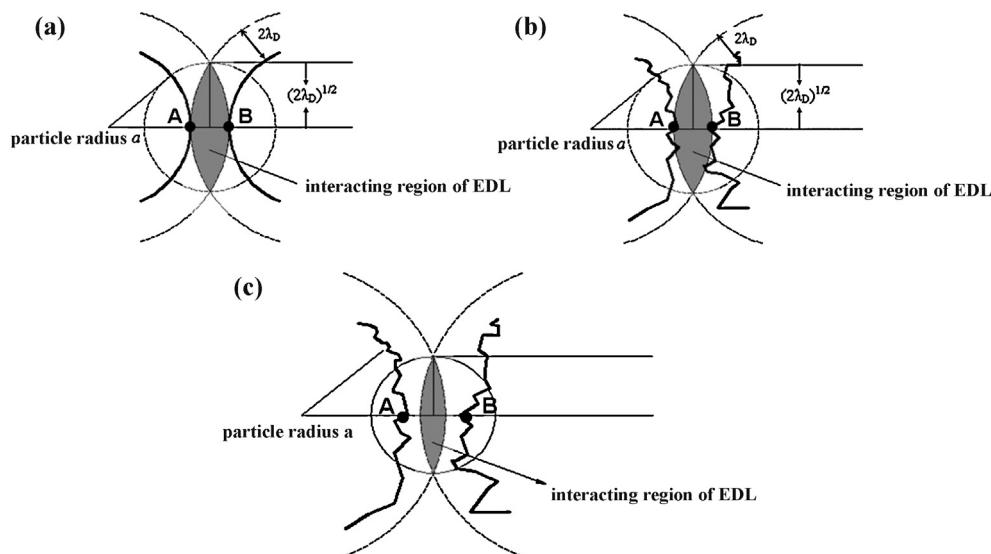


**Fig. 7.** Interfacial electrokinetic models: (a) smooth particles, (b) rough particles, and (c) rough particles after extracting thiophene from the model gasoline to interface. EDL: electric double layer.

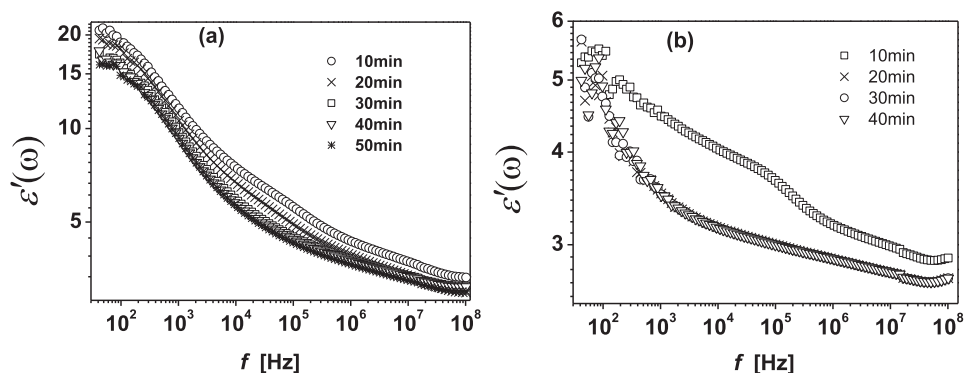


Fig. 8. Dependences of permittivities  $\varepsilon'(\omega)$  spectra of suspensions of (a)  $\text{ZnCl}_2/\text{CMPS-Im(Cl)}$  and (b)  $\text{FeCl}_3/\text{CMPS-Im(Cl)}$  microspheres in model gasoline on extraction time.

are surrounded by CuCl-based imidazolium ILs where these ILs are a type of organic salts with melting points around or below ambient temperature. Meanwhile, the static permittivity values of 10–25 of imidazolium ILs had been reported by Weingärtner in 2006 [57,58], and Weingärtner et al. also showed that static permittivities of 8–15 for imidazolium ILs were compatible with the number densities and dipole moments of the constituent ions. Therefore, the values (in the range 7.57–8.83) of permittivities ( $\varepsilon_p$ ) of dispersed microspheres with 250–300  $\mu\text{m}$  radii are reasonable.

### 3.3.2. Dependences of permittivity spectra of M/CMPS-Im(Cl) ( $M = \text{ZnCl}_2$ and $\text{FeCl}_3$ ) microspheres in model gasoline on extraction time

Dependences of permittivity  $\varepsilon'(\omega)$  spectra of suspensions of  $\text{ZnCl}_2/\text{CMPS-Im(Cl)}$  and  $\text{FeCl}_3/\text{CMPS-Im(Cl)}$  microspheres in model gasoline on extraction time are investigated, respectively, as shown in Fig. 8(a) and (b). We can observe that the dielectric properties of suspensions of M/CMPS-Im(Cl) microspheres in model gasoline are directly disappeared when the extraction time is longer than 20 min, however, the dielectric property of suspensions of CuCl/CMPS-Im(Cl) microspheres (shown in Fig. 4) is existed at all times (from 10 min to 6 h) although it is kept invariant when the extraction time is longer than 50 min. The reason for this phenomenon is possibly ascribed to the different spatial configurations of “hairy surfaces” of M/CMPS-Im(Cl) ( $M = \text{CuCl}$ ,  $\text{ZnCl}_2$  and  $\text{FeCl}_3$ ) microspheres in model gasoline. This investigation will be further studied in the future.

## 4. Conclusion

Real-time dielectric measurements in the frequency range from 40 MHz to 110 MHz are performed for extracting thiophene from model gasoline using M/CMPS-Im(Cl) ( $M = \text{CuCl}$ ,  $\text{ZnCl}_2$  and  $\text{FeCl}_3$ ) microspheres ILs as extractant.

First, it can be observed that dielectric properties of M/CMPS-Im(Cl) ( $M = \text{ZnCl}_2$  and  $\text{FeCl}_3$ ) microspheres in model gasoline are disappeared when the extraction time is longer than 20 min, yet, the dielectric property of CuCl/CMPS-Im(Cl) microspheres in model gasoline exists and maintains invariant from 50 min to 6 h. The reason for this phenomenon is ascribed to the different spatial configurations of “hairy surfaces” of M/CMPS-Im(Cl) ( $M = \text{CuCl}$ ,  $\text{ZnCl}_2$  and  $\text{FeCl}_3$ ) microspheres in model gasoline. Second, the classical counterion polarization in the electric double layer does not appear in this frequency field for all samples, and we suggest that the hard diffusion of counterions into the model gasoline is responsible for this phenomenon. Meanwhile, one dielectric relaxation at MHz is determined to be closely related to the interfacial polarization, the interfacial polarization is ascribed to the buildup of charges on the interfaces between model gasoline and CMPS-supported ILs in

the form of optimized spatial configurations of N-methylimidazole group and its counterions.

For suspensions of CuCl/CMPS-Im(Cl) microspheres in model gasoline, the values of  $\beta$  for all samples are much smaller than 1, which is because the required time to restore the equilibrium charge distribution of surface of dispersed particles is different for imidazolium (Im) group and its corresponding counterions. As a result, it indicates that the investigated system is much different from the non-conducting particles in aqueous solution that always investigated. Meanwhile, dielectric parameters  $\Delta\varepsilon$  and  $\tau_0$  sharply decrease with the increment of extractive time within 50 min, then both of them keep invariant with the increment of extractive time, simultaneously. The reason for this phenomenon is that more and more thiophene is extracted from model gasoline to the surfaces of dispersed particles when the extractive time is increasing. And two factors are responsible for this extractive process: the  $\pi$ -complexation bond ( $d-\pi^*$  back-donation of electrons from 3d orbitals of copper (I) to  $\pi^*$  orbitals of thiophene) and  $\pi-\pi$  interaction (between thiophene and the imidazole rings of ILs). It can be concluded that these two factors result in the decrement of electron density (namely, the polarization strength) on surface of CuCl/CMPS-Im(Cl) microspheres in model gasoline, correspondingly, the result magnified by dielectric parameters is that  $\Delta\varepsilon$  and  $\tau_0$  sharply decrease with the increment of extraction time within 50 min. Meanwhile, this result magnified by a part of phase parameters is:  $\varepsilon_p$  decreases, however,  $\kappa_p$  and  $\kappa_a$  increase with the increment of extraction time. According to the interfacial electrokinetic model for densely packed sediments, the distance between two particles becomes larger when thiophene is extracted from model gasoline to the surfaces of two particles. Correspondingly, this phenomenon magnified by phase parameter is that volume fraction  $\phi$  of CuCl/CMPS-Im(Cl) microspheres in model gasoline of per unit volume decreases with the increment of extraction time. Finally, coupled with interfacial electrokinetic model and the related reports of investigation of static permittivities of imidazolium ILs, it shows that the phase parameters ( $\phi$ ,  $\kappa_m$ ,  $\varepsilon_p$  and  $\kappa_p$ ) calculated by Hanai equations are reasonable.

In conclusion, it should be emphasized that the contribution of new data and dielectric analysis on the interactions and dynamics of extracting thiophene from model gasoline is represented by means of DRS, the information obtained by analyzing the investigated system maybe provide the experimental database or theoretical reference to ILs extraction field. The further investigation is undergoing by our group.

## Acknowledgements

This work was financially supported by the National Nature Science Foundation of China (Nos. 21003074, 21176121, 21173025



and 20976015), and the Natural Science Fund for Colleges and Universities in Jiangsu Province (09KJB530002).

## References

- [1] F. Kremer, Broadband dielectric spectroscopy and its applications, *Dielectrics Newsletter* (March) (1994) 3.
- [2] F. Kremer, A. Schonhals, *Broadband Dielectric Spectroscopy*, Springer-Verlag, Berlin, 2002.
- [3] J. Lyklema, *Fundamentals of interface and colloid science Solid-Liquid Interfaces*, vol. II, Academic Press, New York, 1995.
- [4] A. Delgado, *Interfacial electrokinetics and electrophoresis Surfactant Science Series*, vol. 106, Marcel Dekker, New York, 2002 (Chapters 1 and 3).
- [5] S. Mashimo, T. Umehara, S. Kuwabara, S. Yagihara, Dielectric study on dynamics and structure of water bound to DNA using a frequency range  $10^7$ – $10^{10}$  Hz, *Journal of Physical Chemistry* 93 (1989) 4963–4967.
- [6] N. Miura, N. Asaka, N. Shinyashiki, S. Mashimo, Microwave dielectric study on bound water of globule proteins in aqueous solution, *Biopolymers* 34 (1994) 357–364.
- [7] T. Ishida, T. Makino, Microwave dielectric relaxation of bound water to silica, alumina, and silica–alumina gel suspensions, *Journal of Colloid and Interface Science* 212 (1999) 144–151.
- [8] J.C. Maxwell, *A Treatise on Electricity and Magnetism*, 3rd ed., Clarendon Press, Oxford, 1891.
- [9] K.W. Wagner, Erklärung der dielectricischen nachwirkungsvorgänge auf grund maxwellscher vorstellungen, *Archiv für Elektrotechnik* 2 (1914) 371–387.
- [10] C.T. O’Konski, Electric properties of macromolecules. V. Theory of ionic polarization in polyelectrolytes, *Journal of Physical Chemistry* 64 (1960) 605–619.
- [11] G. Schwarz, A theory of the low-frequency dielectric dispersion of colloidal particles in electrolyte solution, *Journal of Physical Chemistry* 66 (1962) 2636–2642.
- [12] S.S. Dukhin, V.N. Shilov, *Dielectric Phenomena and the Double Layer in Dispersed Systems and Polyelectrolytes*, Wiley, New York, 1974.
- [13] V.N. Shilov, S.S. Dukhin, Theory of low-frequency dispersion of dielectric permittivity in suspensions of spherical colloidal particles due to double-layer polarization, *Colloid Journal* 32 (1970) 293–300.
- [14] M.L. Jiménez, G.J. Arroyo, F. Carrique, U. Kaatz, Broadband dielectric spectra of spheroidal hematite particles, *Journal of Physical Chemistry B* 107 (2003) 12192–12200.
- [15] K.S. Zhao, Z. Chen, An investigation on the high-frequency dielectric dispersion of concentrated ion-exchange resin beads suspensions, *Journal of Colloid and Interface Science* 284 (2006) 1147–1154.
- [16] K. Asami, Dielectric relaxation in a water-oil-triton X-100 microemulsion near phase inversion, *Langmuir* 21 (2005) 9032–9037.
- [17] Z. Chen, K.S. Zhao, Dielectric analysis of macroporous anion-exchange resin beads suspensions, *Journal of Colloid and Interface Science* 276 (2004) 85–91.
- [18] K.J. He, K.S. Zhao, Dielectric analysis of a nanoscale particle in an aqueous solution of low electrolyte concentration, *Langmuir* 21 (2005) 11878–11887.
- [19] M.J. Han, K.S. Zhao, Effect of volume fraction and temperature on dielectric relaxation spectroscopy of suspensions of PS/PANI composite microspheres, *Journal of Physical Chemistry C* 112 (2008) 19412–19422.
- [20] F. Bordini, C. Cametti, Occurrence of an intermediate relaxation process in water-in-oil microemulsions below percolation: the electrical modulus formalism, *Journal of Colloid and Interface Science* 237 (2001) 224–229.
- [21] W. Schrader, S. Halstenberg, R. Behrends, U. Kaatz, Critical slowing in lipid bilayers, *Journal of Physical Chemistry B* 107 (2003) 14457–14463.
- [22] W. Bai, K.S. Zhao, H.L. Mi, Dielectric spectroscopy of Anabaena 7120 protoplast suspensions, *Bioelectrochemistry* 69 (2006) 49–57.
- [23] H.P. Schwan, G. Schwarz, J. Maczuk, H. Pauly, On the low-frequency dielectric dispersion of colloidal particles in electrolyte solution, *Journal of Physical Chemistry* 66 (1962) 2626–2635.
- [24] F. Carrique, L. Zurita, A.V. Delgado, Correlation of the dielectric and conductivity properties of polystyrene suspensions with zeta potential and electrolyte concentration, *Journal of Colloid and Interface Science* 166 (1994) 128–132.
- [25] M.R. Gittings, D.A. Saville, Electrophoretic mobility and dielectric response measurements on electrokinetically ideal polystyrene latex particles, *Langmuir* 11 (1995) 798–800.
- [26] F.J. Arroyo, A.V. Delgado, F. Carrique, M.L. Jiménez, T. Bellini, F. Mantegazza, Effect of ionic mobility on the enhanced dielectric and electro-optic susceptibility of suspensions: theory and experiments, *Journal of Chemical Physics* 116 (2002) 10973–10980.
- [27] R.W. O’Brien, The response of a colloidal suspension to an alternating electric field, *Advances in Colloid and Interface Science* 16 (1982) 281–320.
- [28] J. Lyklema, S.S. Dukhin, M.M. Springer, V.N. Shilov, The relaxation of the double layer around colloidal particles and the low-frequency dielectric dispersion: Part I. Theoretical considerations, *Journal of Electroanalytical Chemistry* 143 (1983) 1–21.
- [29] C. Grosse, K.R. Foster, Permittivity of a suspension of charged spherical particles in electrolyte solution, *Journal of Physical Chemistry* 91 (1987) 3073–3076.
- [30] V.N. Shilov, A.V. Delgado, F. González-Caballero, C. Grosse, Thin double layer theory of the wide-frequency range dielectric dispersion of suspensions of non-conducting spherical particles including surface conductivity of the stagnant layer, *Colloids and Surfaces A: Physicochemical and Engineering Aspects* 192 (2001) 253–265.
- [31] C.S. Mangelsdorf, L.R. White, Dielectric response of a dilute suspension of spherical colloidal particles to an oscillating electric field, *Journal of the Chemical Society, Faraday Transactions* 93 (1997) 3145–3154.
- [32] J.J. López-García, J. Horno, A.V. Delgado, F. González-Caballero, Use of a network simulation method for the determination of the response of a colloidal suspension to a constant electric field, *Journal of Physical Chemistry B* 103 (1999) 11297–11307.
- [33] R.T. Yang, A. Takahashi, F.H. Yang, New sorbents for desulfurization of liquid fuels by  $\pi$ -complexation, *Industrial and Engineering Chemistry Research* 40 (2001) 6236–6239.
- [34] A.J. Hernández-Maldonado, R.T. Yang, Desulfurization of diesel fuels by adsorption via  $\pi$ -complexation with vapor-phase exchanged Cu(I)-Y zeolites, *Journal of the American Chemical Society* 126 (2004) 992–993.
- [35] R.T. Yang, A.J. Hernández-Maldonado, F.H. Yang, Desulfurization of transportation fuels with zeolites under ambient conditions, *Science* 301 (2003) 79–81.
- [36] A.B.S.H. Salem, Naphtha desulfurization by adsorption, *Industrial and Engineering Chemistry Research* 33 (1994) 336–340.
- [37] A.B.S. Salem, H.S. Hamid, Removal of sulfur compounds from naphtha solutions using solid adsorbents, *Chemical Engineering and Technology* 20 (1997) 342–347.
- [38] S. Velu, X. Ma, C. Song, Selective adsorption for removing sulfur from jet fuel over zeolite-based adsorbents, *Industrial and Engineering Chemistry Research* 42 (2003) 5293–5304.
- [39] X.M. Wang, H. Wan, M.J. Han, L. Gao, G.F. Guan, Removal of thiophene and its derivatives from model gasoline using polymer-supported metal chlorides ionic liquid moieties, *Industrial and Engineering Chemistry Research* 51 (2012) 3418–3424.
- [40] P. Somasundaran, T.W. Healy, D.W. Fuerstenau, Surfactant adsorption at the solid-liquid interface-dependence of mechanism on chain length, *Journal of Physical Chemistry* 68 (1964) 3562–3566.
- [41] T. Hanai, H.Z. Zhang, K. Sekine, K. Asaka, K. Asami, The number of interfaces and the associated dielectric relaxations in heterogeneous systems, *Ferroelectrics* 86 (1988) 191–204.
- [42] A. Ishikawa, T. Hanai, N. Koizumi, Evaluation of relative permittivity and electrical conductivity of ion-exchange beads by analysis of high-frequency dielectric relaxations, *Japanese Journal of Applied Physics* 20 (1981) 79–86.
- [43] K. Asami, A. Irimajiri, T. Hanai, N. Koizumi, A method for estimating residual inductance in high frequency A.C. measurements, *Bulletin of the Institute for Chemical Research, Kyoto University* 51 (1973) 231–245.
- [44] K.S. Cole, R.H. Cole, Dispersion and absorption in dielectrics I: alternating current characteristics, *Journal of Chemical Physics* 9 (1941) 341–351.
- [45] M.L. Jiménez, F.J. Arroyo, J.V. Turnhout, A.V. Delgado, Analysis of the dielectric permittivity of suspensions by means of the logarithmic derivative of its real part, *Journal of Colloid and Interface Science* 249 (2002) 327–335.
- [46] M. Wübbenhorst, J.V. Turnhout, Conduction free dielectric loss  $de/d \ln(f)$  – a powerful tool for the analysis of strong (ion) conduction materials, *Dielectrics Newsletter* 1–6 (2000) 1956–1959.
- [47] K. Asami, Characterization of heterogeneous systems by dielectric spectroscopy, *Progress in Polymer Science* 27 (2002) 1617–1659.
- [48] T. Hanai, T. Imakita, N. Koizumi, Analysis of dielectric relaxations of W/O emulsions in the light of theories of interfacial polarization, *Colloid and Polymer Science* 260 (1982) 1029–1034.
- [49] T. Hanai, Theory of dielectric dispersion due to the interfacial polarization and its application to emulsions, *Kolloid-Zeitschrift* 171 (1960) 23–31.
- [50] D.A.G. Bruggeman, Berechnung verschiedener physikalischer konstanten von heterogenen substanzen, *Annalen der Physik* (Leipzig) 24 (1935) 636–679.
- [51] A.J. Hernandez-Maldonado, F.H. Yang, G. Qi, R.T. Yang, Desulfurization of transportation fuels by  $\pi$ -complexation sorbents: Cu(I)-, Ni(II)-, and Zn(II)-zeolites, *Applied Catalysis B* 56 (2005) 111–126.
- [52] N.H. Ko, J.S. Lee, E.S. Huh, H.L. Lee, K.D. Jung, H.S. Kim, M. Cheong, Extractive desulfurization using Fe-containing ionic liquids, *Energy and Fuels* 22 (2008) 1687–1690.
- [53] J.D. Holbrey, W.M. Reichert, M. Nieuwenhuyzen, O. Sheppard, C. Hardacre, R.D. Rogers, Liquid clathrate formation in ionic liquid-aromatic mixtures, *Chemical Communications* 4 (2003) 476–477.
- [54] B.M. Su, S.G. Zhang, Z.C. Zhang, Structural elucidation of thiophene interaction with ionic liquids by multinuclear NMR spectroscopy, *Journal of Physical Chemistry B* 108 (2004) 19510–19517.
- [55] A.J. Hernández-Maldonado, R.T. Yang, Desulfurization of transportation fuels by adsorption, *Catalysis Reviews* 46 (2004) 111–150.
- [56] J. Lyklema, H.P. van Leeuwen, M. Minor, DLVO-theory, a dynamic reinterpretation, *Advances in Colloid and Interface Science* 83 (1999) 33–69.
- [57] H. Weingärtner, The static dielectric constant of ionic liquids, *Zeitschrift für Physikalische Chemie* 220 (2006) 1395–1405.
- [58] H. Weingärtner, P. Sasisanker, C. Daguenet, P.J. Dyson, I. Krossing, J.M. Slattery, T. Schubert, The dielectric response of room-temperature ionic liquids: effect of cation variation, *Journal of Physical Chemistry B* 111 (2007) 4775–4780.